YMTHE, Volume *25*

Supplemental Information

The Circular RNA Interacts with STAT3, Increasing Its Nuclear Translocation and Wound Repair by Modulating Dnmt3a and miR-17 Function

Zhen-Guo Yang, Faryal Mehwish Awan, William W. Du, Yan Zeng, Juanjuan Lyu, De Wu, Shaan Gupta, Weining Yang, and Burton B. Yang

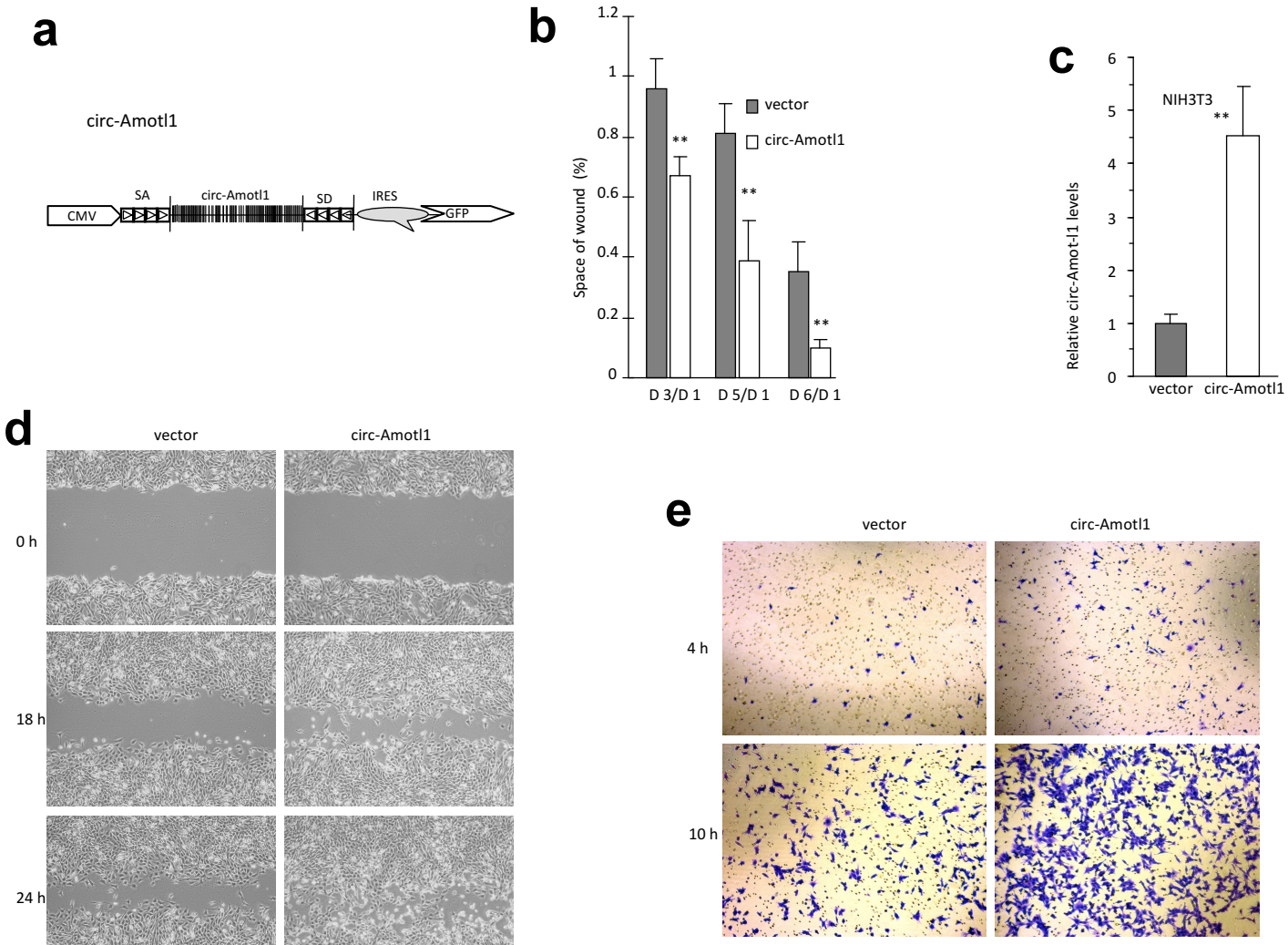

Fig S1. circ-Amotl1 enhanced wound healing and migration

(a). Structure of circ-Amotl1

(b) The ratio of wound sizes on the third, fifth and sixth days to that on the first day indicated faster wound healing process in the circ-Amotl1-injected side. ** *p<0.01,* Error bars, ±S.D, *n=10*.

(c) RNAs extracted from NIH3T3 cells transfected with circ-Amotl1 were subject to RT and real-time PCR to detect circ-Amotl1 levels. Significant increase in circ-Amotl1 levels was detected in the circ-Amotl1-transfected cells. ** *p <0.01.* Error bars, S.D (*n=4*).

(d) Upper, Scratch wound healing assay was performed to measure the motility of NIH3T3 cells transfected with circ-Amotl1 and control vector. Overexpression of circ-Amotl1 enhanced cell migration. Lower, Quantitaion of the migration. ** *p <0.01.* Error bars, S.D (*n=5*).

(e) Typical pictures of trans-well migration assay.

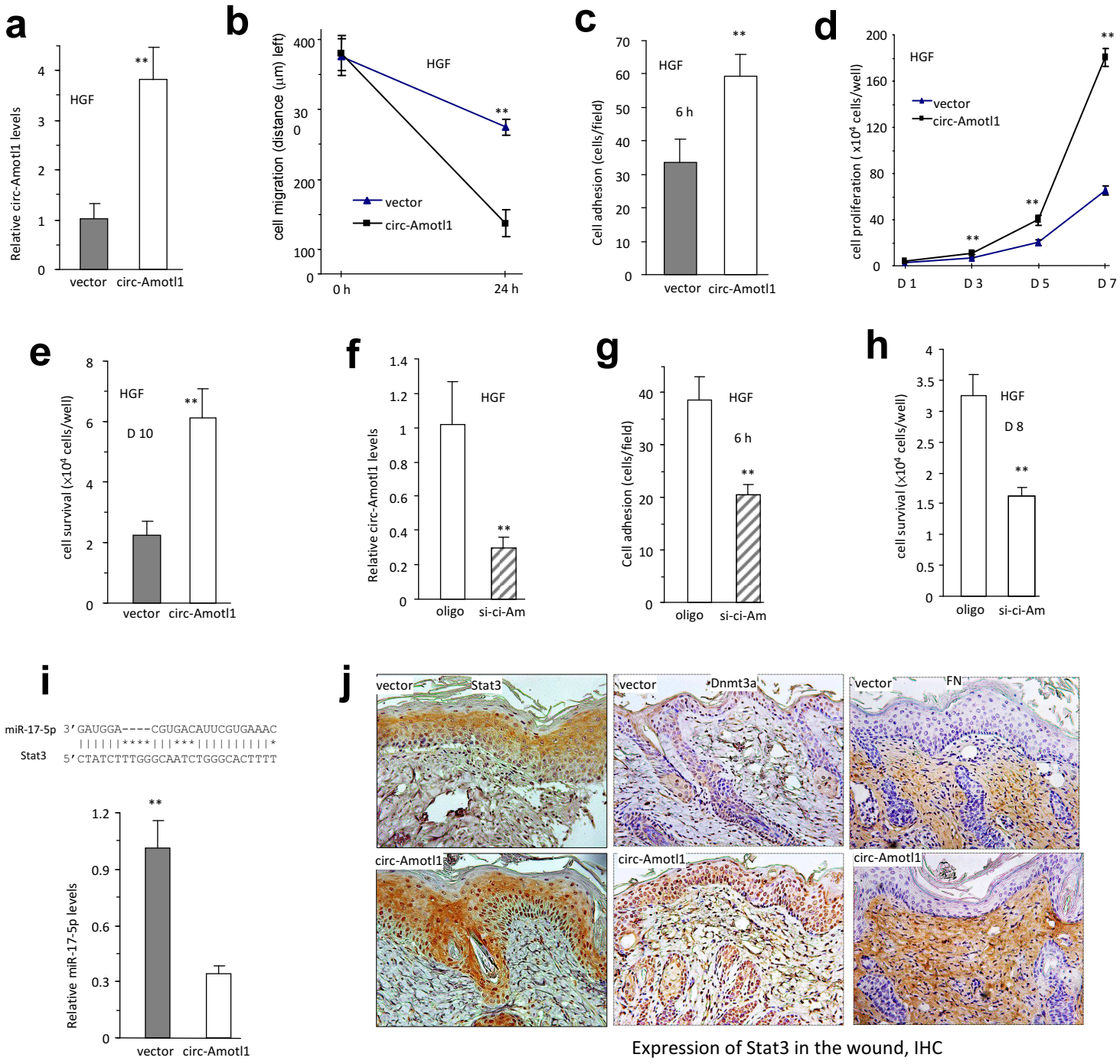

Fig S2. circ-Amotl1 enhanced cell proliferation, migration, and survival

(a) RNAs extracted from HGF cells transfected with circ-Amotl1 or control vector were subject to real-time PCR. Up-regulation of circ-Amotl1 was detected in the circ-Amotl1-transfected cells. ** *p<0.01.* Error bars, S.D (*n=4*).

(b) Wound healing assay showed that overexpression of circ-Amotl1 increased migration of the HGF cells. ** *p <0.01,* Error bars, S.D (*n=5*).

(c) Overexpression of circ-Amotl1 increased HGF cell adhesion.

(d) Cell proliferation assay showed that HGF cells transfected with circ-Amotl1 proliferated faster than the control. ** *p <0.01,* Error bars, S.D (*n=5*).

(e) Maintained in serum-free medium for 10 days, HGF cells transfected with circ-Amotl1 displayed increase in survival relative to the control. ** *p <0.01,* Error bars, S.D (*n=5*).

(f) Down-regulation of circ-Amotl1 was detected in the siRNA-transfected cells as compared to the control. ***p <0.01,* Error bars, S.D (*n=4*).

(g) Silencing circ-Amotl1 repressed cell adhesion on Petri-dish in HGF cells after 6 h incubation. ** *p <0.01,* Error bars, S.D (*n=5*)

(h) Silencing circ-Amotl1 repressed HGF cell survival after being maintained in serum-free medium for 8 days. ** *p <0.01,* Error bars, S.D (*n=5*).

(i) Ectopic expression of circ-Amotl1 decreased miR-17-5p expression.

(j) Sections of wound tissues from circ-Amotl1- and control plasmid-injected mice were subject to immunohistochemistry staining. Increased expression of Stat3, Dnmt3a, and fibronectin was detected in circ-Amotl1-injected mice.

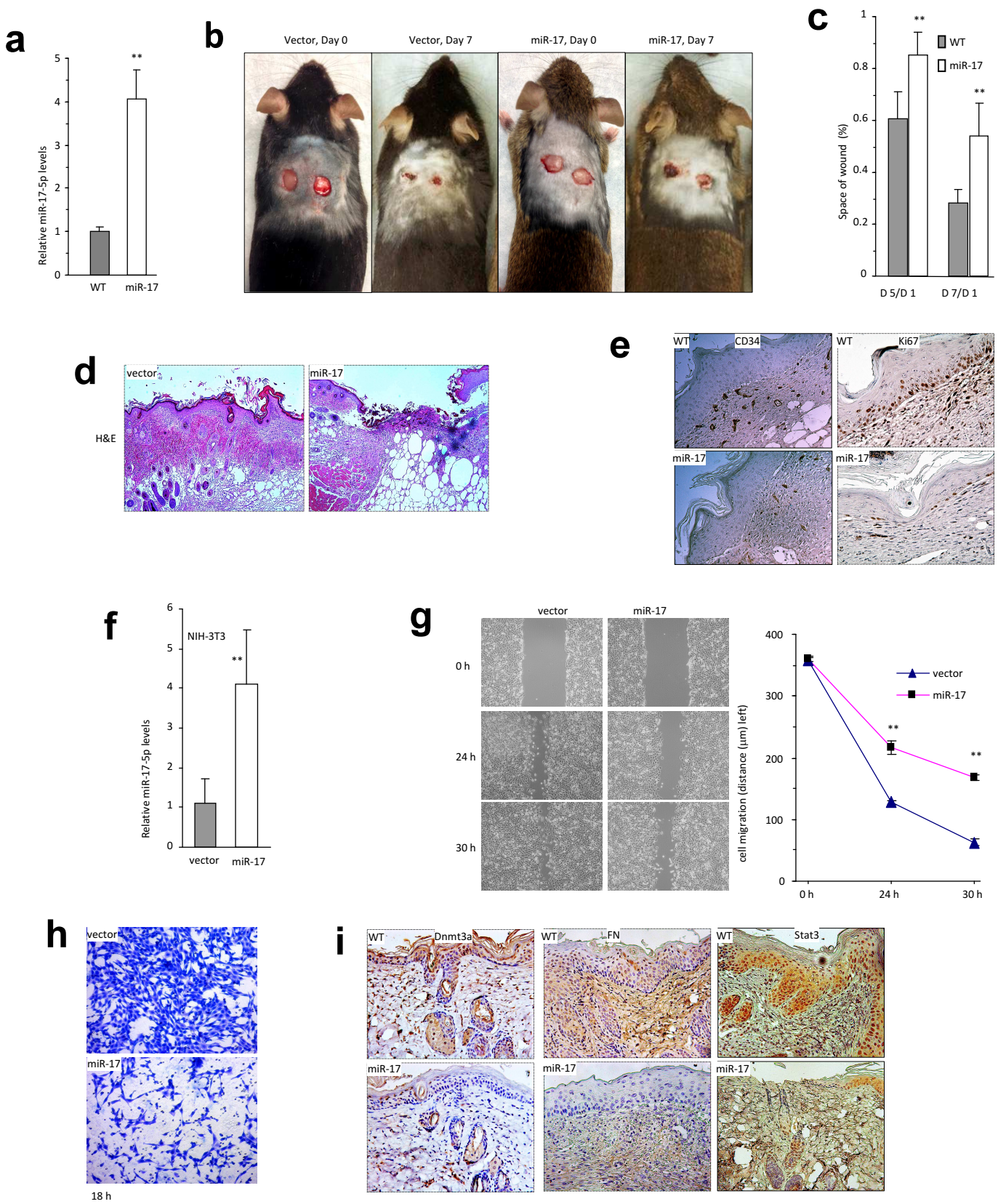

Fig S3. Mutual regulation of circ-Amotl1 and miR-17-5p. **(a)** Wound tissues were subject to real-time PCR to confirm up-regulation of miR-17-5p. **(b)** Typical pictures were taken from seventh day showing that miR-17 transgenic mice had delayed healing compared to the wild-type group. **(c)** After mice were slaughtered, wound size was measured by multiplying longest length by greatest width. The ratio of wound sizes on the fifth and seventh day to that on the first day indicated slower wound healing process in the miR-17 transgenic mice relative to controls. **(d)** Typical pictures of H&E staining showing larger wound in the miR-17 tissue. **(e)** Immunohistochemistry staining of wound tissues showed decreased levels of CD34 (left) and Ki67 (right). **(f)** Cell lines stably transfected with miR-17 or the control vector were subject to real-time PCR to confirm up-regulation of miR-17-5p. **(g)** Left, scratch wound healing assay was performed to measure the motility of NIH3T3 cells transfected with miR-17 and control vector. Overexpression of miR-17 decreased cell migration. Right, Quantitaion of the migration. ** $p < 0.01$. Error bars, S.D ($n=5$). **(h)** Typical picture of trans-well migration assay. **(i)** Typical pictures of immunohistochemistry staining showed decreased expression of Dnmt3a, fibronectin, and Stat3 in the miR-17 transgenic mice.

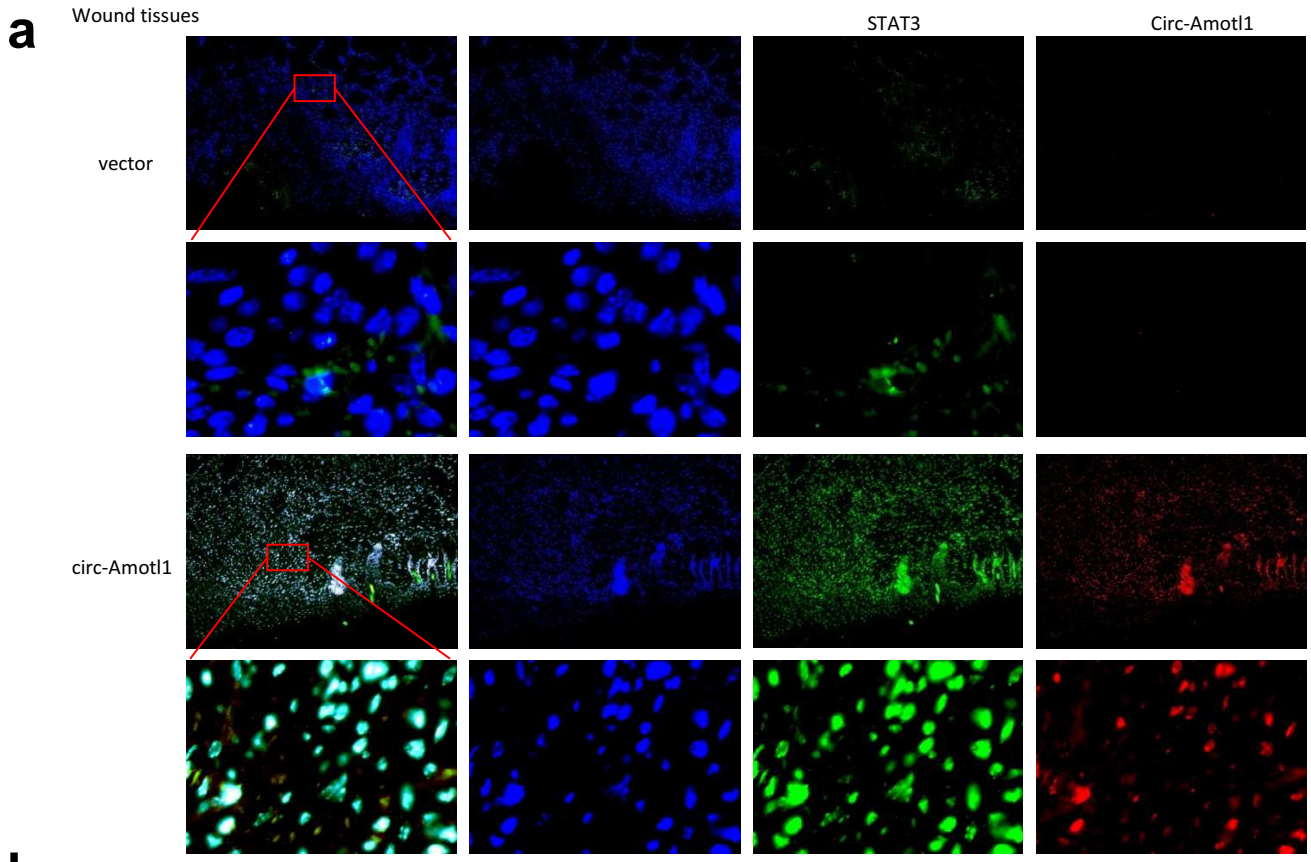

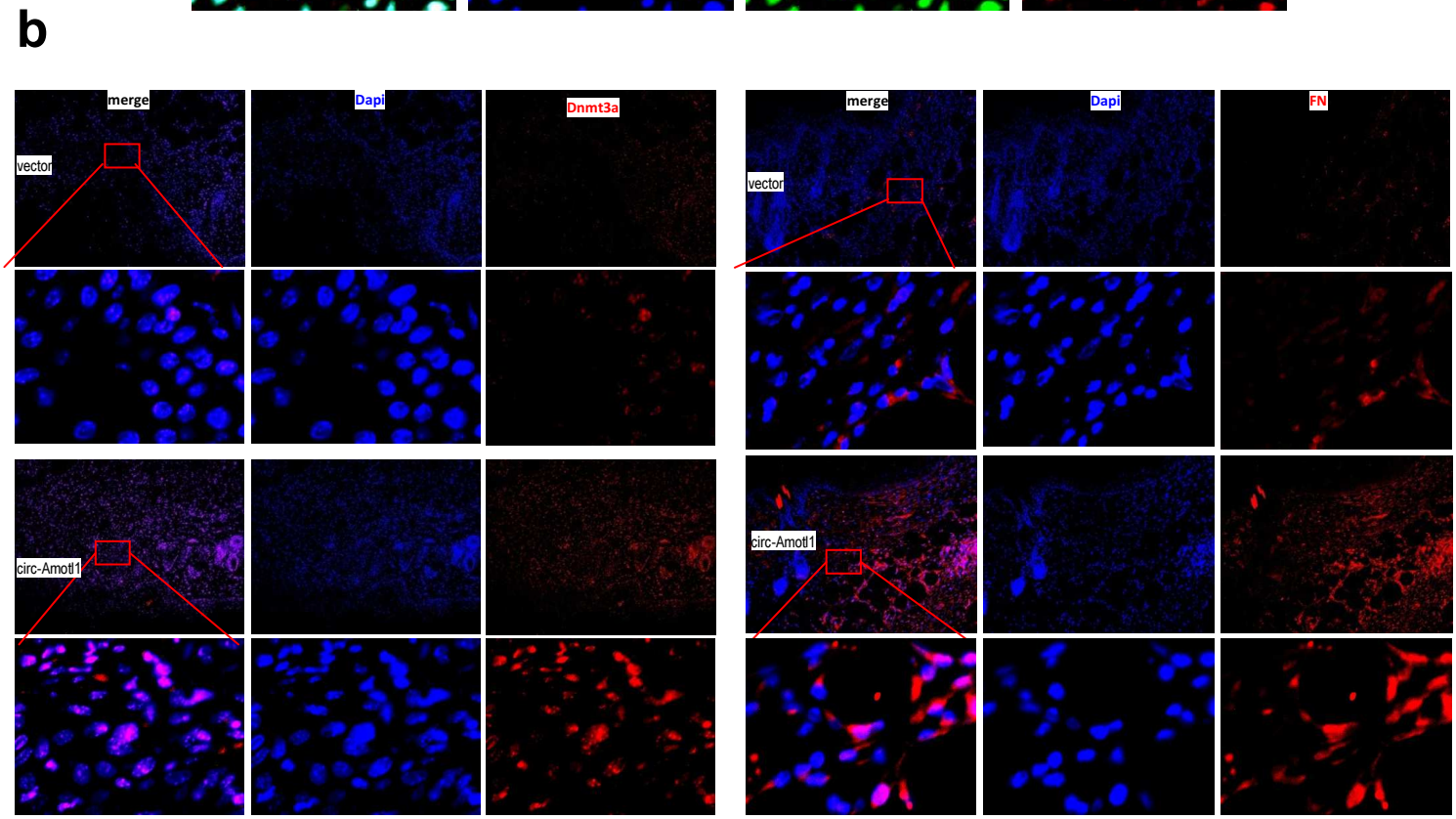

Fig S4. Delivery of circ-Amotl1 in wound tissues increased expression of Stat3, Dnmt3a and fibronectin

(a) The mock- and circ-Amotl1-injected tissues were stained with DAPI (blue), Stat3 (green), and circ-Amotl1 (red). High intensity of Stat3 and circ-Amotl1 were detected in the nuclei.

(b) The mock- and circ-Amotl1-transfected injected tissues were stained with DAPI and Dnmt3a (red, left) or fibronectin (red, right). High intensity of Stat3 and fibronectin were detected in the circ-Amotl1-injected tissues.

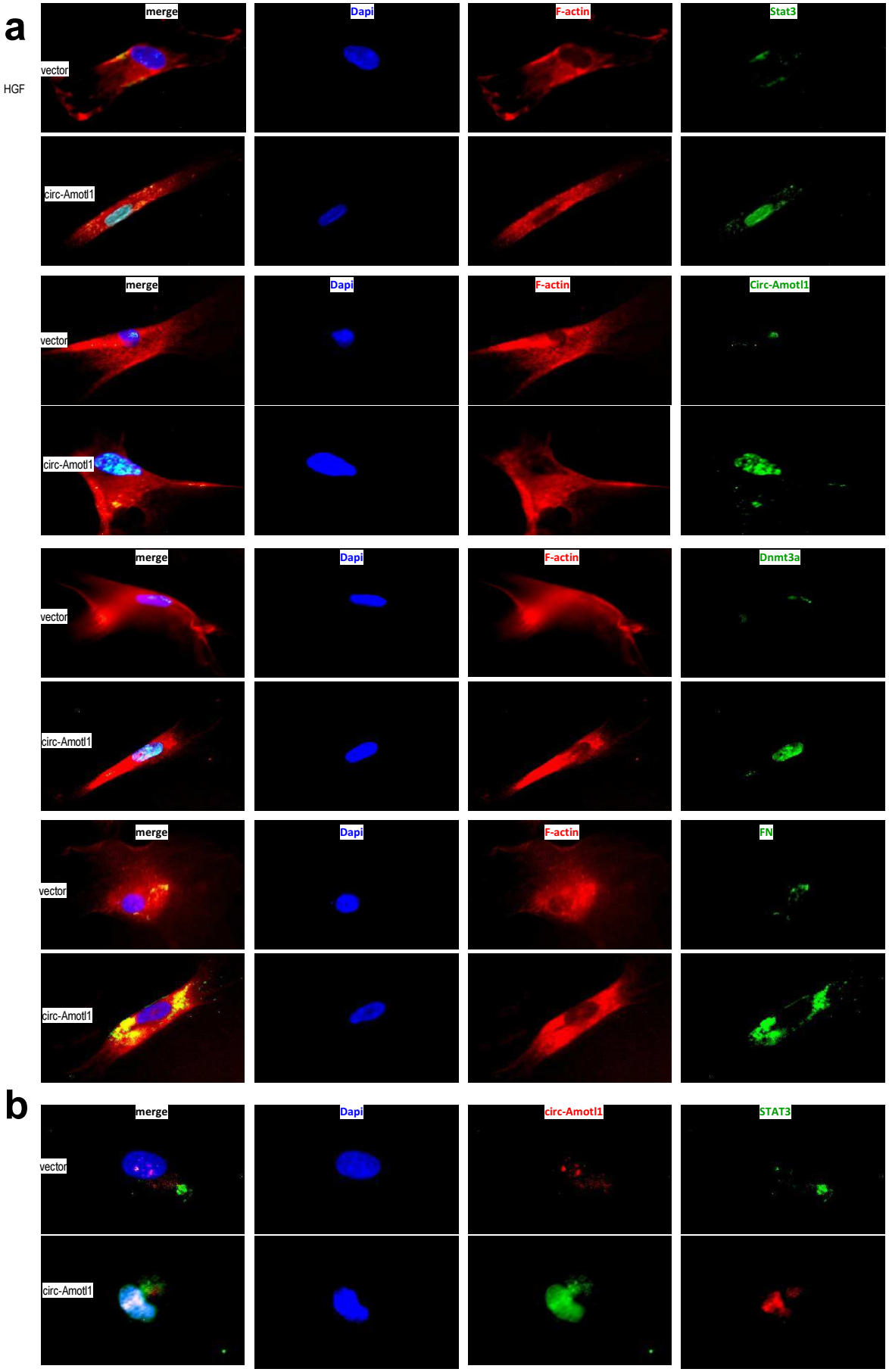

Fig S5. Expression of circ-Amotl1 in HGF cells increased expression of Stat3, Dnmt3a and fibronectin. (a) The mock- and circ-Amotl1-transfected HGF cells were stained with DAPI (blue), F-actin (red) and Stat3, Dnmt3a, fibronectin, or in situ hybridized with circ-Amotl1 (green). Increased expression of these molecules was detected in the circ-Amotl1-transfected cells. (b) The cells were stained with DAPI (blue), circ-Amotl1 (green), and Stat3 (red). Co-localization of circ-Amotl1 and Stat3 was detected in the circ-Amotl1-transfected cells.

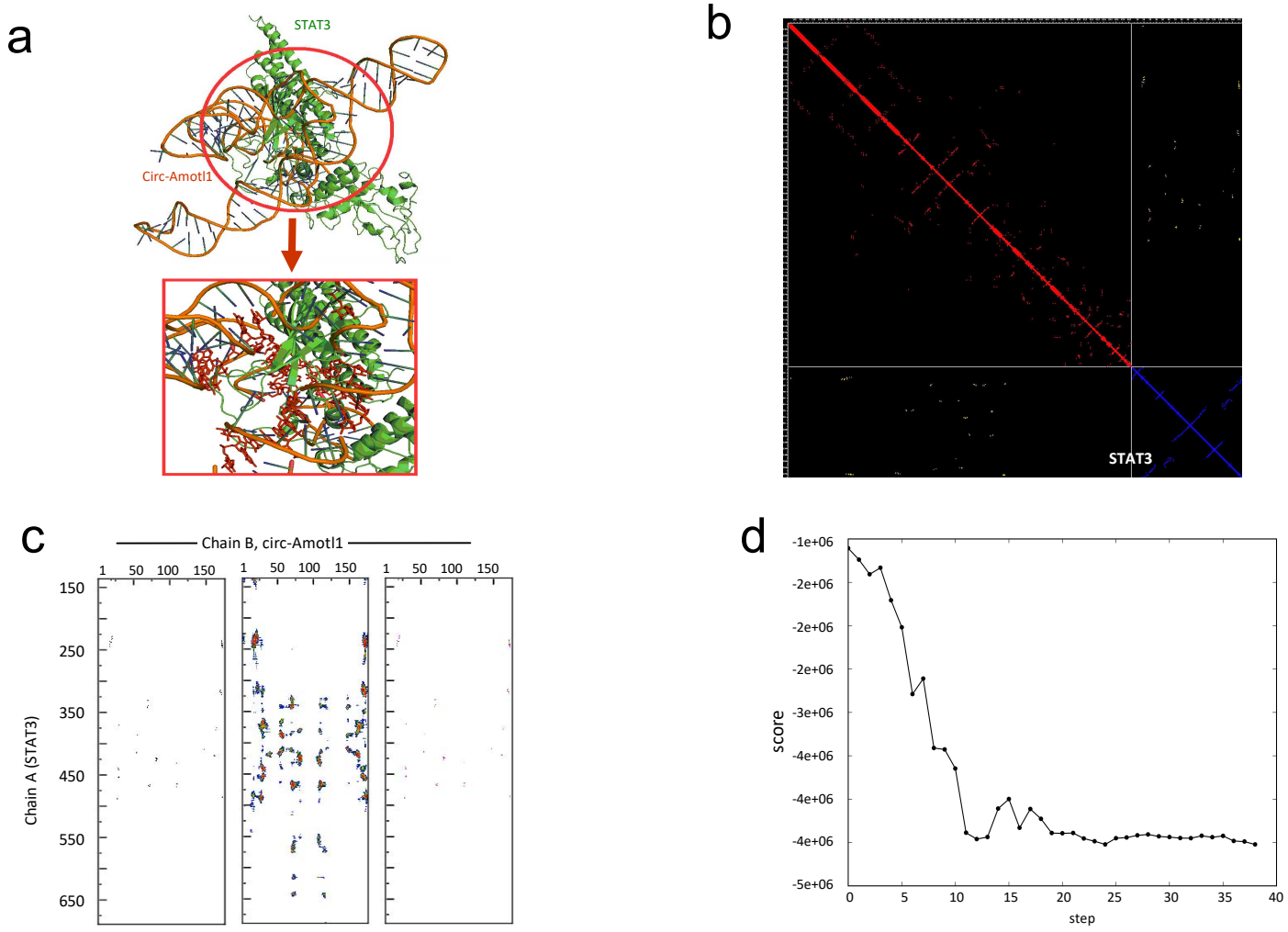

e

name	sequence
27.38.hu.Cir.Amotl1-R	5′ ggtt ggggt gcc ata ccgc ag ttg
27.39.hu.Cir.Amotl1-F	5′ cagcctgtgagaacagatgtggcc
28.76.hu.Amotl1-F	5′ cgcctcatgtggagggcaaagttg
28.77.hu.Amotl1-R	5′ ccct gatg ctac tggttg cctcca
27-77.musDnmt3a-SacI	5′ ccc gagctc gggctgggatcagtggccaatagg
27-78.musDnmt3a-MluI	5′ cc acgcgt acc ttg tcaaa gaaaaag caa gaa
26.27mus.Stat3-F	5′ ccgacccaggtagtgctgc
26.28.mus.Stat3-R	5′ caatggtattgctgcaggtcg
25-66.musFN1-F	5′ gaagacagatgagcttcccca
25-67.musFN1-R	5′ ggttggtgatgaaggggtc
21-60.hsa-miR-17-5p	5′caaagtgcttacagtgcag
circ-Amotl1 probe	5′ caaagaggatcttcaactcgttaccccatact
Blocking oligo	5'cggaacctctcatttccacctctgagatcctcaggaagtttgggg agtggaagttacaaagaggatcttcaactcgttaccccatact
control oligo	5' tccttcctctctttctctcccttgtga
siRNA	5′ GGGGUAACGAGUUGAAGAUUU 5′ AUCUUCAACUCGUUACCCCUU

Fig S6. Computational analysis of circ-Amotl1 interacting with Stat3

(a) Graphic three-dimensional structures of the docking models of circ-Amotl1 with Stat3.
(b) The contact map in the binding residues between circ-Amotl1 and Stat3.
(c) The residue-level resolution contact maps in the binding residues between circ-Amotl1 and Stat3.
(d) Refinement of the best docked circ-Amotl1-Stat3 model showing MC score vs. steps of simulation.
(e) Primer sequences used for the study.

Table S1. The circ-Amotl1-STAT3 Distance

N(res No)	atom	chain	AA (res No)	atom	chain	distance	type
LYS 140	NZ	A	A 18	O3′	B	2.3	Phil phil
LYS 140	NZ	A	A 19	OP1	B	2.75	Phil phil
GLU 229	O	A	U 21	OP1	B	3.47	Phil phil
TYR 230	O	A	C 20	OP2	B	1.69	Phil phil
TYR 230	OH	A	A 19	O2′	B	2.02	Phil phil
LYS 233	CD	A	C 20	O3′	B	2.37	Phil phil
LYS 233	CE	A	U 21	OP2	B	0.33	Phil phil
THR 234	N	A	C 20	OP2	B	2.44	Phil phil
THR 234	OG1	A	A 19	O3′	B	2.6	Phil phil
THR 236	O	A	A 170	O4′	B	1.47	Phil phil
ASP 237	OD1	A	A 170	OP1	B	2.74	Phil phil
ASP 237	O	A	U 17	OP2	B	2.43	Phil phil
GLU 238	OE1	A	A 18	O3′	B	2.83	Phil phil
GLU 238	OE2	A	C 20	OP1	B	3.1	Phil phil
GLU 238	OE1	A	A 19	C5′	B	0.84	Phil phil
LEU 240	O	A	A 170	N3	B	1.51	Phob phil
ALA 241	CB	A	A 170	O2′	B	1.58	Phob phil
ALA 241	O	A	A 171	O4′	B	3.42	Phob phil
ASP 242	OD1	A	U 17	C2	B	1.39	Phil phil
TRP 243	CE3	A	A 170	N1	B	1.95	Phil phil
TRP 243	CZ3	A	A 171	N1	B	2.86	Phil phil
LYS 244	CB	A	A 171	C4	B	1.42	Phil phil
LYS 244	CG	A	A 170	C2	B	1.68	Phil phil
ARG 245	CB	A	U 17	C5	B	3.28	Phil phil
ARG 245	N	A	A 171	N3	B	3.3	Phil phil
GLN 247	OE1	A	A 171	N1	B	2.76	Phil phil
GLN 248	OE1	A	A 171	O2′	B	3	Phil phil
ASN 315	OD1	A	G 168	O3′	B	2.57	Phil phil
ASN 315	OD1	A	U 169	OP1	B	1.96	Phil phil
LYS 318	NZ	A	G 168	C4′	B	2.08	Phil phil
SER 319	OG	A	U 169	O3′	B	3.41	Phil phil
SER 319	OG	A	A 170	OP1	B	3.48	Phil phil
VAL 322	CG1	A	A 170	N6	B	3.39	Phob phil
MET 331	SD	A	U 69	O2′	B	2.52	Phob phil
HIS 332	CE1	A	C 70	C5′	B	2.74	Phil phil
HIS 332	NE2	A	U 69	O3′	B	2.96	Phil phil
LYS 340	NZ	A	C 70	OP2	B	2.41	Phil phil
GLY 342	O	A	U 69	OP1	B	2.84	Phob phil
VAL 343	CG2	A	U 69	OP1	B	1.97	Phob phil
LYS 370	CE	A	C 30	OP2	B	1.5	Phil phil
LYS 370	CB	A	C 29	OP1	B	3.01	Phil phil
ASP 371	OD2	A	C 30	N4	B	3.41	Phil phil
SER 372	OG	A	C 28	OP2	B	2.57	Phil phil
VAL 373	O	A	A 163	OP2	B	2.61	Phob phil
ARG 379	NH1	A	U 162	OP1	B	3.08	Phil phil
ASN 385	OD1	A	G 54	OP1	B	3	Phil phil

Table S1. The circ-Amotl1-STAT3 Distance (con.)

N(res No)	atom	chain	AA (res No)	atom	chain	distance	type
ASN 385	CB	A	U 55	OP1	B	3.19	Phil phil
LEU 387	CD2	A	U 55	OP2	B	3.37	Phob phil
HIS 410	ND1	A	C 146	O2′	B	2.84	Phil phil
ARG 414	NH1	A	G 54	OP2	B	2.78	Phil phil
GLU 415	O	A	G 54	OP1	B	3.45	Phil phil
GLN 416	CD	A	A 160	OP1	B	2.69	Phil phil
GLY 419	CA	A	A 160	O2′	B	2.45	Phob phil
ASN 420	N	A	A 160	O2′	B	2.73	Phil phil
ASN 420	ND2	A	G 161	C4′	B	0.4	Phil phil
ARG 423	NH1	A	G 80	C4′	B	1.61	Phil phil
ARG 423	O	A	G 81	C5′	B	2.04	Phil phil
ASN 425	O	A	G 81	C4′	B	2.35	Phil phil
ASN 425	N	A	C82	OP1	B	3.44	Phil phil
CYS 426	CA	A	G 81	O2′	B	3.07	Phil phil
ALA 428	CB	A	G 80	O2′	B	3.22	Phob phil
ALA 428	N	A	G 81	O4′	B	3.15	Phob phil
ILE 431	CG2	A	G 107	O2′	B	2.73	Phob phil
VAL 432	CG1	A	U 109	OP2	B	3.35	Phob phil
VAL 432	CG2	A	A 108	O3′	B	2.92	Phob phil
LEU 438	CD1	A	C 28	C5′	B	1.69	Phob phil
THR 440	OG1	A	C 28	O3′	B	2.48	Phil phil
THR 440	CG2	A	C 29	C5′	B	1.57	Phil phil
GLU 442	OE1	A	C 30	OP1	B	0.43	Phil phil
GLU 442	CD	A	C 29	O3′	B	1.94	Phil phil
ASP 453	OD2	A	C 30	O2′	B	3.05	Phil phil
GLU 455	OE1	A	C 30	C6	B	3.26	Phil phil
GLU 455	OE2	A	C 29	O4′	B	0.48	Phil phil
HIS 457	ND1	A	C 28	O2′	B	2.38	Phil phil
SER 465	OG	A	C 110	OP1	B	2.94	Phil phil
SER 465	OG	A	U 109	OP2	B	3.13	Phil phil
ASN 466	ND2	A	G 72	O6	B	2.63	Phil phil
ILE 467	CG2	A	C 71	OP2	B	0.47	Phob phil
ILE 467	CD1	A	C 70	OP1	B	1.8	Phob phil
CYS 468	CB	A	G 72	OP2	B	3.04	Phil phil
CYS 468	N	A	C 71	OP2	B	3	Phil phil
GLN 469	NE2	A	U 109	OP1	B	1.31	Phil phil
GLN 469	NE2	A	A 108	O3′	B	3.23	Phil phil
ASN 485	O	A	C 172	P	B	2.4	Phil phil
ASN 485	O	A	A 171	O3′	B	1.63	Phil phil
ASN 486	CA	A	C 172	OP2	B	1.18	Phil phil
ASN 486	CA	A	A 171	O3′	B	3.23	Phil phil
PRO 487	N	A	C 172	OP1	B	1.05	Phob phil
PRO 487	CD	A	A 171	O3′	B	2.44	Phob phil
LYS 488	CD	A	C 28	O4′	B	3.04	Phob phil
LYS 488	NZ	A	U 27	C2	B	0.49	Phil phil
LYS 488	NZ	A	C 172	O2′	B	3.18	Phil phil
ASN 489	N	A	U 27	O2′	B	3.26	Phil phil

The table reporting a list of atoms “in contact” (within the distance cutoff) with relative distances less than 3.5Å.

Table S2. Accessible Surface Area table of circ-Amolt1-Stat3 complex

Buried area upon the complex formation (A^2) 6316.2
Buried area upon the complex formation (%) 11.13
Interface area (A^2) 3158.1
Interface area STAT3 (%) 11.77
Interface area circ-AMOTL1 (%) 10.56
POLAR Buried area upon the complex formation (A^2) 2667.0
POLAR Interface (%) 42.22
POLAR Interface area (A^2) 1333.5
NON POLAR Buried area upon the complex formation (A^2) 3649.2
NON POLAR Interface (%) 57.78
NON POLAR Interface area (A^2) 1824.6
Residues at the interface_total (n) 148
Residues at the interface_STAT3 96
Residues at the interface_circ-AMOTL1 52

Table S3. circ-Amolt1-Stat3 interaction overview

Number of interacting residues STAT3 **60**
Number of interacting residues circ-AMOTL1 **32**
Number of hydrophilic-hydrophobic interaction **20**
Number of hydrophilic-hydrophilic interaction **73**
Number of hydrophobic-hydrophobic interaction **0**